Experimental and numerical investigations of Tesla turbine

IOP Conf. Series: Journal of Physics: Conf. Series **1101** (2018) 012029 doi:10.1088/1742-6596/1101/1/012029

Experimental and numerical investigations of Tesla turbine

K Rusin[1], W Wróblewski[1] and M Strozik[1]

[1]Silesian University of Technology, Konarskiego 18, 44-100 Gliwice, Poland

E-mail: krzysztof.rusin@polsl.pl

Abstract. Tesla turbine is a bladeless turbine and its principle of operation is based on shear stress arising from fluid viscosity and turbulence. A prototype of Tesla turbine is an object of numerical and experimental investigations presented in the paper. Experimental investigations were carried out for different inlet pressures and compared to results from numerical investigations. The roughness of the disc surface was measured and taken into account in the numerical analysis. Numerical investigations were performed in CFX 17.1 commercial software for steady state and transient. Comparison of power and efficiency vs rotational velocity characteristics shows relatively good agreement between experiment and CFD.

1. Introduction

Tesla turbine, known also as a bladeless turbine or boundary layer turbine, was invented in 1913 by Nikola Tesla [1]. It is a radial turbine, whose rotor consists of multiple discs, mounted in parallel on the shaft. Its principle of operation is based on shear stresses arising from fluid viscosity and turbulence. The supply system consists of one or multiple nozzles. Their aim is to accelerate working medium and to deliver it at an optimal angle [2]. Fluid flows tangentially to the surface of the disc from the outer to the inner radius and due to adhesive forces, sticks to it. Tangential stresses occur on the disc surface due to momentum diffusion, which is an effect of fluid viscosity and makes disc rotating.

Advantages [3,4] like resistance to erosion, flexibility in the choice of working medium and reversibility of flow make bladeless turbine well suited for systems powered by renewable energy sources with the low boiling medium [5]. Structure of the turbine is unsophisticated, which means low costs of manufacturing. Consequently, the economic viability of an installation with Tesla turbine is good.

Tesla turbine has been often an object of investigations. Kim and Yoon [6] investigated the possibility of using a bladeless expander in a cogeneration installation supplied with waste heat. Song et al. [7] tested the influence of low boiling medium on Tesla turbine performance. Carey [8] analysed a 4kW solar cogeneration system and developed a mathematical model in order to determine its optimal working conditions. Schosser et al [9] conducted numerical investigation of flow in the rotor and compared the results with data obtained from analytical solution.

Preliminary experimental investigation of Tesla turbine and comparison of performance with the prediction of numerical analysis is presented in the paper. The object of interest was Tesla turbine model MK3 manufactured by Gyroscope company. The experiment involves the determination of rotor disc roughness, efficiency characteristic of the generator and finally power and efficiency vs rotational velocity characteristics. Numerical investigations are performed with the use ANSYS 17.1 package: Meshing and CFX.

2. Experimental investigations set up

Experimental investigations were performed in Institute of Power Engineering and Turbomachinery in the Silesian University of Technology. Test stand, which is presented in Figure 1, was divided into two parts: (a) supply system and (b) measurement system.

a) b)

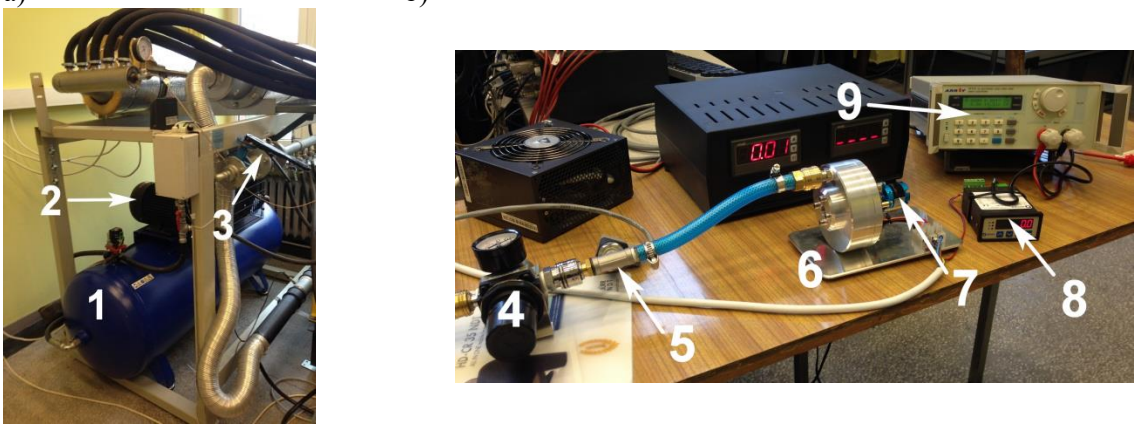

Figure 1. Test stand: (a) supply system and (b) measurement system

The supply system consisted of air tank (1) with 0.5 m^3 volume, reciprocating compressor (2) and two valves (3, 4). The aim of this system was to produce air flow with demanded parameters. The compressor was filling the tank with the air up to pressure 8 bar. The outflow from the tank was regulated by means of two valves and was carried out through the duct of 13 mm in inner diameter. The main valve (3) served as a safety valve and could quickly cut off the flow. The membrane control valve (4) was supposed to stabilize the pressure level and keep it constant. Steady state, which is required to perform series of measurements, occurs as long as pressure upstream of the valve is higher than the set value, owing to which time for measurement is relatively short (e.g. 1 minute). The second part was measurement system. A pressure transducer (5) was placed right after the control valve, which allowed control of inlet pressure to the Tesla turbine (6). No loss was assumed in the short duct between pressure transducer and turbine, so pressure value obtained from transducer was considered as an inlet pressure to the turbine. The turbine was connected to the generator (7). The generator was brushless motor model HC 2816-1220, which is often used in flying radio controlled models. It was connected to the tachometer (8), which was supposed to measure rotational velocity of generator and turbine. Its principle of operation was based on counting impulses produced in the generator, where every 3 impulses corresponded to 1 revolution. Electric load (9) was responsible for loading generator with demanded value. It was possible to set either resistance or exact power value. The electric load measured also power produced in the generator.

In order to make a valid comparison between CFD analysis and experimental investigations, it was necessary to obtain the same quantity that is internal power. Internal power is an effect of thermodynamic processes taking place in turbine nozzles and in a rotor and does not take into account losses in bearings or in the generator. This quantity can be obtained in CFD calculations, but in case of experimental investigations only electrical power is measured directly. Therefore it is necessary to estimate the efficiency of generator and power lost in bearings due to friction. It was assumed that efficiency of bearings is equal to 99%, but to obtain efficiency characteristic of the generator, the test rig was designed.

The test rig is presented in Figure 2. A power supply (1) produced electric current with proper voltage and amperage, which propelled electric motor (2). The rotational velocity of the motor was changing with the use of the potentiometer (3). The electric motor was connected to the investigated generator (4). Efficiency characteristic of the motor was given by the manufacturer, so the shaft power propelling the generator was known. The generator was loaded by the electric load (5), which forced the exact

value of produced power. As in the main test stand, the rotational velocity was measured by the tachometer (6). The electric current produced in generator was rectified in (7). The measurement procedure was based on efficiency estimation with respect to rotational velocity and applied electric load. It was possible to estimate efficiency by measuring power propelling the motor and power produced in the generator.

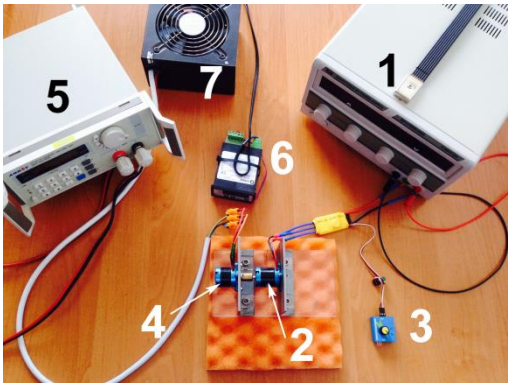

Figure 2. Generator test rig

Figure 3. Taylor-Hobson Surtronic 3+ Roughness Gage

The roughness of the disc surface is of significant importance for the turbine performance. It may cause an increase of turbulence in the boundary layer and therefore increase of shear stresses occurring on disc walls. In order to make CFD analysis more precise, it is recommended to determine this parameter. The roughness of disc surface was measured with the use of Taylor-Hobson Surtronic 3+ Roughness Gage, which is presented in Figure 3. Two sides of the one rotor disc were surveyed. The measurement was carried out along 5 radii crossing outlet sections of the rotor and in two directions: parallel and normal with respect to the radius. The length of the measuring section totalled 0.8 mm. As the result, roughness expressed as arithmetical mean deviation R_a was obtained. R_a was calculated from the equation:

$$R_a = \frac{1}{a}\sum_{i=1}^{a}|h_i| \tag{1}$$

Where:
h – roughness height
a – number of measurements

Results obtained from experiments are presented in section “Results”.

3. Numerical analysis

The numerical analysis was performed in ANSYS 17.1 commercial software. The computational mesh was generated using ANSYS Meshing tool and the setup of numerical model was done in CFX. This software uses an implicit finite volume formulation to resolve discretized unsteady Reynolds-averaged Navier-Stokes equations. Computations were performed both in steady state and in transient.

3.1. Model of geometry

Geometry model, presented in Figure 4, was reflecting dimensions of Tesla turbine model, which was investigated experimentally. For simplicity reasons, only half of the turbine was modelled that is two inter-disc gaps and the gap between the last disc and the turbine casing. Such configuration takes into consideration two discs and one side of the third disc and does not influences the results of numerical

simulations, but decreases computational time. The inter discs gaps were 73mm in diameter and 1.5 mm thick and the discs were 1.3 mm thick. The spacers of spiral shape were also taken into account. The rotor domain was supplied by the inlet system, which consisted of cylindrical chamber (1) with two inlet orifices with 1.8mm in diameter (2) providing the working medium directly in between the discs. The chamber was 6mm in diameter, 13mm in length and was positioned at an angle 45° with respect to the vertical symmetry axis of the rotor. Tip clearance (3) between the rotor and the casing was 0.5 mm in height. The outlet from the rotor consisted of 5 orifices with 7.5 mm in diameter, whose centres were located 10mm away from the rotor axis. The working medium flowed out from the rotor to the converging collecting chamber (4) which was linked by four cylindrical ducts (5) with second converging collecting chamber (6). Outflow into the ambient took place by means of 20mm length duct (7) with 13 mm in diameter.

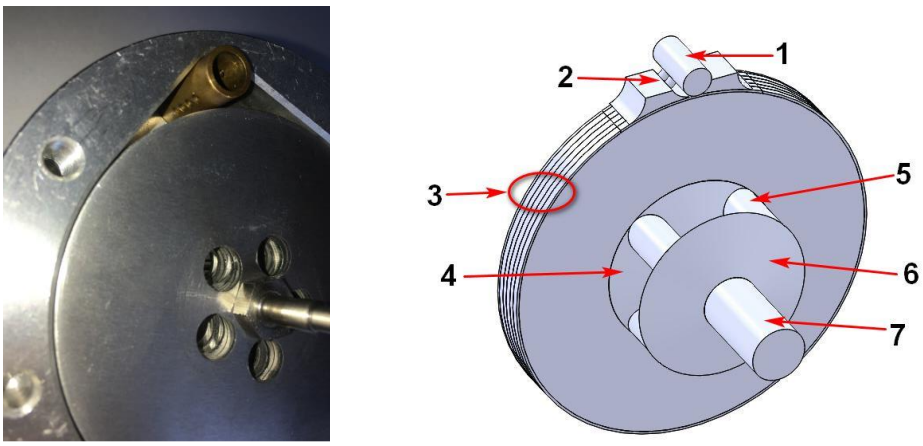

Figure 4. The geometry of the numerical model

3.2. Numerical model and boundary conditions

Numerical simulations were performed for air treated as an ideal gas. Changes in laminar fluid viscosity due to temperature changes were taken into consideration, as it may influence shear stresses occurring on disc walls. It was modelled with the use of Sutherland formula [10]:

$$\mu(T) = \mu_{ref}\left(\frac{T}{T_{ref}}\right)^{3/2}\frac{T_{ref}+T_S}{T+T_S} \tag{2}$$

where: Sutherland temperature T_S=110.4 K, reference viscosity μ_{ref}=1.719·10^{-5} Pa·s, reference temperature T_{ref}=273.15 K. Turbulence model used for simulations was k-ω SST [11], which is a combination of k-ω turbulence model near the wall and k-ε turbulence model in the far field. The roughness of the surface was modelled using sand grain roughness ε. It can be derived using arithmetical mean deviation of roughness height R_a [12]:

$$\varepsilon = \frac{2R_a}{\left(\frac{\pi}{2} - cos^{-1}\left(1-\frac{\pi^2}{16}\right)^{\frac{1}{2}} - \frac{\pi}{4}\left(1-\frac{\pi^2}{16}\right)^{\frac{1}{2}}\right)} \tag{3}$$

Sand grain roughness was calculated according to results obtained from measurement of roughness. Details of the numerical model and boundary conditions are presented in Figure 5. Total pressure and total temperature were assumed at the inlet sections of the supplying chamber. Inlet pressure was equal

to 3 or 4 bar and the total temperature was equal to 303 K. Two inlet sections ensured equal conditions for both inlet orifices, which is the case for whole turbine geometry. The supply system and the tip clearance domains were stationary, but bottom walls of the tip clearance, which were in contact with the discs, were rotating. Tip clearance was connected to the inlet system and to the rotor with General Grid Interface. Symmetry boundary condition was applied on one lateral wall of the tip clearance. The rotor domain was modelled as stationary, but lateral walls were rotating. Additionally, sand grain roughness and no-slip wall were applied on these walls. Spacer domains were rotating and connected to the rotor with frozen rotor interface. The outlet system was modelled as stationary, thus it was connected to spacer domain with frozen rotor interface. Static pressure equal to 1 bar was assumed at the outlet section. All walls of the model were adiabatic.

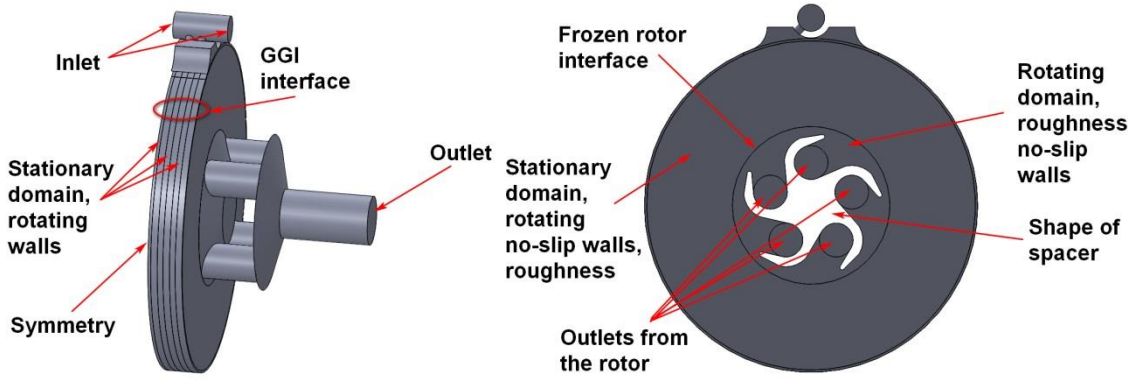

Figure 5. Details of the numerical model

Conservation equations for mass, momentum and energy were solved:

$$\frac{\partial \rho}{\partial t} + \nabla \cdot (\rho \mathbf{v}) = 0 \tag{4}$$

$$\frac{\partial (\rho \mathbf{v})}{\partial t} + \nabla \cdot (\rho \mathbf{v} \otimes \mathbf{v}) = -\nabla p + \nabla \cdot \boldsymbol{\tau} \tag{5}$$

$$\frac{\partial (\rho h_{tot})}{\partial t} - \frac{\partial p}{\partial t} + \nabla \cdot (\rho \mathbf{v} h_{tot}) = \nabla \cdot (\lambda \nabla T) + \nabla \cdot (\mathbf{v} \cdot \boldsymbol{\tau}) \tag{6}$$

These equations were discretized in space with the use of the high-resolution scheme. Integration with respect to time was done using implicit second-order Euler scheme.

Sensitivity study of mesh density influence on results was performed. 5 numerical meshes with 2M, 2.7M, 4.1M, 5.2 M and 7.7 M elements were created and value of power was treated as an indication of mesh quality. Sensitivity study of time step for transient simulations was performed as well.
Results of mesh sensitivity study and numerical simulations are presented in paragraph “Results”.

4. Results

Results of roughness measurement are presented in Figure 6. Roughness in all directions is small and the differences with the change of direction are insignificant. Average roughness totals R_a=0.28μm, which proves that surface was improved with polishing. Such a small value roughness has minor contribution to increase of turbulence viscosity and thereby generated power.

Characteristic of generator efficiency with respect to produced power and rotational velocity is presented in Figure 7. Characteristic is of paraboloid shape with maximum efficiency equal to 84% achieved for 18000 min^{-1} and 65 W. Region of efficiency higher than 70% is limited by 25-80W range and 10000-25000 min^{-1} range. The rapid drop in efficiency occurs for higher rotational velocities i.e. above 27500 min^{-1} and for small power values.

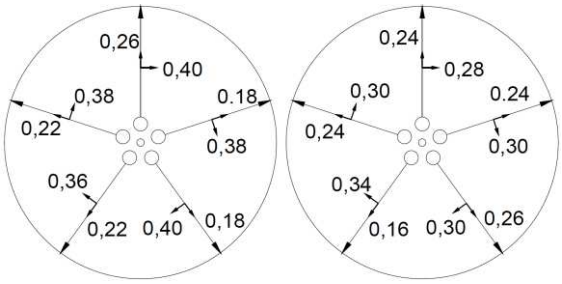

Figure 6. Results of disc roughness measurement

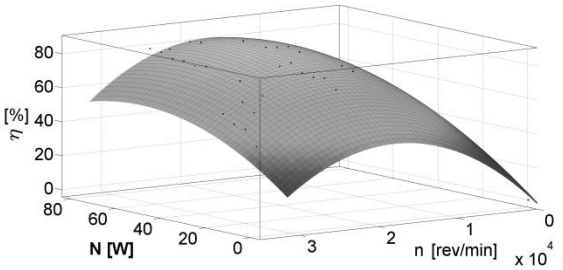

Figure 7. Characteristic of generator efficiency with respect to power and rotational velocity

The efficiency of the generator can be estimated using the equation:

$$\eta = 104.2 - 0.003869n + 0.8053N + 2.052 \cdot 10^{-5} n \cdot N + 3.9 \cdot 10^{-8} n^2 - 0.00978N^2 \qquad (7)$$

Results of mesh independence study are presented in Figure 8. Reference power N_{ref} was obtained from the highest density mesh, to which other results were compared. Analysis proved that mesh with 4.1M does not influence results. Fragment of discretization is presented in Figure 9. Areas with highest velocity gradient, i.e. the supply system and the upper part of the inter-disc gap have the finest mesh. Boundary layer was created on disc walls, cylindrical chamber, two inlet orifices, the upper wall of tip clearance, two collecting chambers and walls of 4 cylindrical linkers. It provided distribution of non-dimensional distance $y^+ \leq 1$. Time step equal to 10^{-5}s was determined for transient computations.

Comparisons of power and efficiency characteristics for experiment and numerical investigations are presented respectively in Figure 10 and Figure 11. Power in numerical investigations was calculated basing on averaging power values from each time step of the transient simulation. All characteristics of power are of a parabolic shape and relatively flat, which means that in a wide range of rotational velocity power changes insignificantly, e.g. for 3 bar CFD power varies only 25% of maximal value. Values obtained from numerical investigations are higher than values obtained from the experiment.

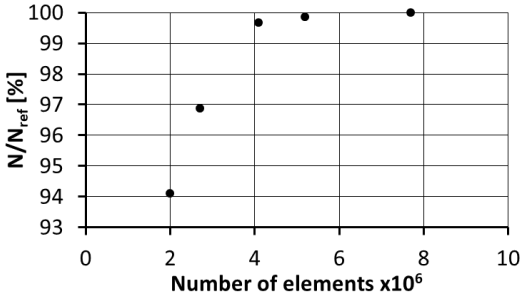

Figure 8. Analysis of mesh independence study

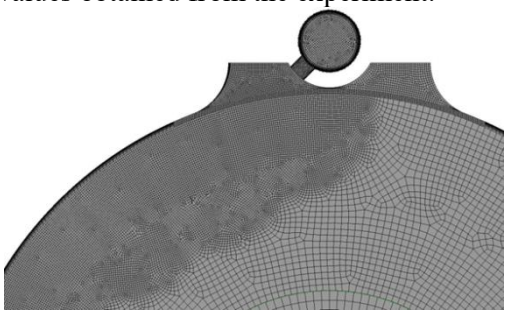

Fig. 9 Model discretization

Maximal power values are: 55.6 W (25000 min^{-1}) for 3 bar CFD, 42.5 W (20500 min^{-1}) for 3 bar experiment, 98.3 W (30000 min^{-1}) for 4 bar CFD and 71.5 W (20500 min^{-1}) for 4 bar experiment. Efficiency was calculated using equation:

$$\eta = \frac{N}{\dot{m} \cdot T_{in} \cdot c_p \left(1 - \left(\frac{p_{out}}{p_{in}} \right)^{\left(\frac{\kappa - 1}{\kappa} \right)} \right)} \qquad (8)$$

where: $\dot{m}$ – mass flow, T_{in} – inlet temperature, c_p – specific heat capacity at constant pressure, $p_{in,out}$ – pressure at inlet and outlet, κ – heat capacity ratio. Mass flow for the experiment was estimated assuming choked flow in the inlet orifices. Maximal efficiency values correspond to maximal power and are equal

to: 11.2 % for 3 bar CFD, 8.4% for 3 bar experiment, 11.8% for 4 bar CFD and 8.9% for 4 bar experiment. An increase of inlet pressure causes a shift of maximal efficiency toward higher rotational velocities.

Several factors influenced disparities between experimental investigations and CFD analysis. The most important one is precision of turbine manufacturing. Discs are not ideally parallel to each other after mounting on a shaft, therefore the width of the inter-disc gap is not constant. Lack of appropriate sealing of inlet system might cause volumetric loses. It should be also noted that efficiency characteristic of the generator was estimated only for 500-30000 min^{-1} range due to overheating of the electric motor, therefore it is not recommended to use it beyond this range of rotational velocity. However, values obtained from experiment partially exceeded this limit, thus estimation of power can be misleading. It can be seen that for case 4 bar, the higher rotational velocity, the bigger differences between results obtained from CFD and experiment.

Numerical model has its own flawns as well. The biggest challenge comes from flow rotation. Additional body force occurs, which interact with the turbulence [13]. This may lead to false prediction of eddy viscosity and thereby power.

Figure 12 and Figure 13 present Mach number distribution for inlet pressure 4 bar and rotational velocity 30000 min^{-1} obtained from steady-state numerical investigations.

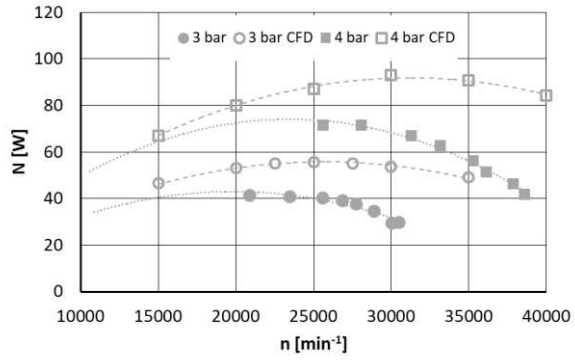

Figure 10. Characteristics of power vs rotational velocity

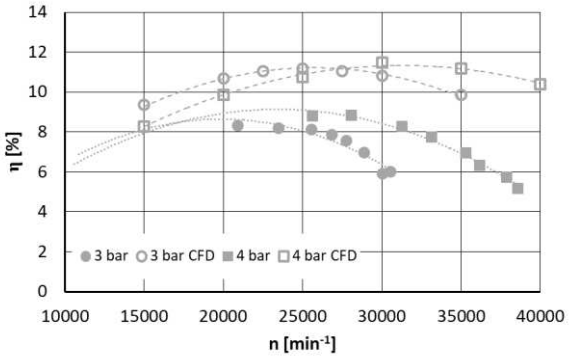

Figure 11. Characteristics of efficiency vs rotational velocity

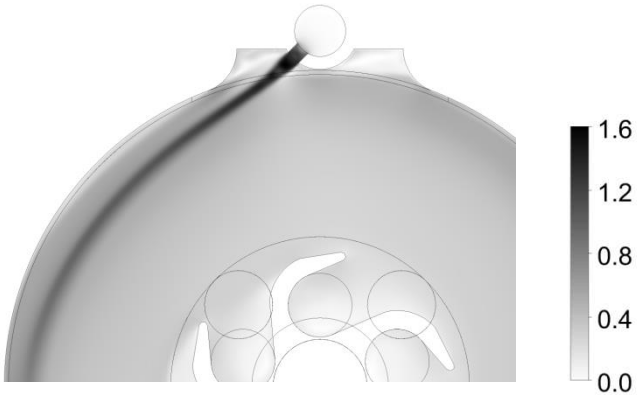

Figure 12. Mach number distribution in the inter-disc gap for 4 bar inlet pressure, n=30000 min^{-1}

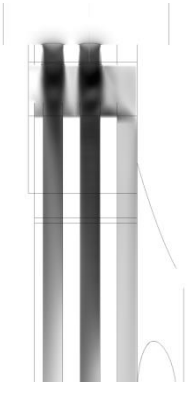

Figure 13. Mach number distribution in the cross-section of an inter-disc gap for 4 bar inlet pressure, n=30000 min^{-1}

It can be seen in Figure 13 that the working medium in the inlet chamber has to perpendicularly change direction, therefore vena contracta occurs in the inlet orifices. Air mainly flows into the inter-disc gaps,

but there is also an interaction with disc tips. The working medium forms a jet flowing out from the inlet, which is visible in Figure 12. The highest Mach number is equal to 1.6 and it occurs at the outlet section from the inlet orifices. The jet flowing into the inter-disc gap is bending due to the occurrence of centrifugal forces coming from rotational velocity. An inlet orifice angle equal to 45° does not provide satisfactory flow path, as the jet flowing to the rotor should be moved as remotely as possible from the outlet. This would ensure higher torque and generated power. Fluid velocity decreases approaching the outlet system, and average Mach number in the outlet orifices is equal to 0.16. The higher fluid velocity at the outlet, the bigger kinematic loss and lower overall turbine efficiency.

5. Conclusions

The paper presents experimental and numerical investigations of Tesla turbine. Three experimental stands were designed. Their aim was to measure generator efficiency, rotor disc roughness and Tesla turbine performance characteristics. Rotor disc roughness equal to R_a=0.28 indicated polished surface, which did not contribute in a significant way to shear stress generation. Maximal power values obtained from experimental investigations performed for inlet pressure 3 and 4 bar were respectively equal to 42.5 W and 71.5 W, which corresponded with efficiency 8.4% and 8.9%. Steady-state and transient numerical investigations were performed in CFX 17.1 commercial software. The numerical model took into account most of the important phenomena, including change of the laminar viscosity with the temperature and disc roughness. Mesh independence study was also performed. Power and efficiency characteristics based on averaged transient results for each time step of transient computations were obtained. The highest power and efficiency values were: 55.6 W, 11.2% for inlet pressure 3 bar and 98.3 W, 11.8% for 4 bar. The highest Mach number was equal to 1.6. An inlet orifice angle should be increased in order to improve turbine performance.

Investigations indicated on challenges associated with measurement of Tesla turbine performance parameters but also revealed turbine potential for low power applications. However, in order to achieve higher efficiency, retooling of the inlet nozzles, as well as the outlet system geometry, has to be done.

Acknowledgements

The presented work was performed within the Silesian University of Technology statutory research funds for young scientists. This research was partially supported by the PL-Grid Infrastructure.

References

[1] Tesla N, *Turbine, Patent No: 1,061,206*, United States Patent Office of New York, 1913
[2] Neckel A L and Godinho M 2015 *Experimental Thermal and Fluid Science* **62** 131
[3] Lampart P and Jędrzejewski ł 2011 *Journal of Theoretical and Applied Mechanics* **49** 447
[4] Sengupta S and Guha A 2012 *Journal of Power and Energy* **226** 650
[5] Lampart P, Kosowski K, Piwowarski M and Jędrzejewski Ł 2009 *Polish Maritime Res.* **63** 28
[6] Kim Ch K and Yoon J Y 2016 *Energy* **101** 411
[7] Song J, Gu Ch and Li X 2018 *Applied Thermal Engineering* **110** 28
[8] Carey V P 2010 *Journal of Engineering for Gas Turbines and Power* **132** 122301-1
[9] Schosser C, Lecheler S and Pfitzner M 2016 *Periodica Polytechnica Mech Eng* **61** 12
[10] Sutherland W 1893 *Philosophical Magazine* **5** 507
[11] Menter F 1993 *24th Fluid Dynamics Conference,* Orlando, USA
[12] Adams T, Grant Ch and Watson H 2012 *Int. J. of Mech. Engineering and Mechatronics* **1** 66
[13] Tucker P G 2013 *Progress in Aerospace Sciences* **63** 1